Pharm Res (2013) 30:1050–1064
DOI 10.1007/s11095-012-0942-y

RESEARCH PAPER

Role of Drug Efflux and Uptake Transporters in Atazanavir Intestinal Permeability and Drug-Drug Interactions

Olena Kis • Jason A. Zastre • Md. Tozammel Hoque • Sharon L. Walmsley • Reina Bendayan

Received: 17 July 2012 / Accepted: 19 November 2012 / Published online: 7 December 2012
© Springer Science+Business Media New York 2012

ABSTRACT

Purpose To investigate the role of membrane-associated drug transporters in regulating the intestinal absorption of the HIV-1 protease inhibitor, atazanavir, and assess the potential contribution of these transporters in clinical interactions of atazanavir with other protease inhibitors and tenofovir disoproxil fumarate (TDF).

Methods Intestinal permeability of atazanavir was investigated *in vitro*, using the Caco-2 cell line system grown on Transwell inserts, and *in situ*, by single-pass perfusion of rat intestinal segments, jejunum and ileum, in the absence or presence of standard transporter inhibitors or antiretroviral drugs.

Results Atazanavir accumulation by Caco-2 cells was susceptible to inhibition by P-glycoprotein and organic anion transporting polypeptide (OATP) family inhibitors and several antiretroviral drugs (protease inhibitors, TDF). The secretory flux of atazanavir (basolateral-to-apical P_{app}) was 11.7-fold higher than its absorptive flux. This efflux ratio was reduced to 1.5–1.7 in the presence of P-glycoprotein inhibitors or ritonavir. P-glycoprotein inhibition also resulted in 1.5–2.5-fold increase in atazanavir absorption *in situ*. Co-administration of TDF, however, reduced atazanavir intestinal permeability by 13–49%, similar to the effect observed clinically.

Conclusions Drug transporters such as P-glycoprotein and OATPs regulate intestinal permeability of atazanavir and may contribute to its poor oral bioavailability and drug-drug interactions with other protease inhibitors and TDF.

KEY WORDS atazanavir · drug transporters · HIV-1 protease inhibitors · intestinal permeability · tenofovir

ABBREVIATIONS

ABC	ATP-binding cassette
ARV	antiretroviral drug
BCRP	breast cancer resistance protein
CYP	cytochrome P450
GF120918	elacridar
HIV	human immunodeficiency virus
MDR	multidrug resistance gene
MPP	1-methyl-4-phenylpyridinium
MRP	multidrug resistance-associated protein
NNRTI	non-nucleoside reverse transcriptase inhibitor
NRTI	nucleoside/nucleotide reverse transcriptase inhibitor
OAT	organic anion transporter
OATP	organic anion transporting polypeptide
OCT	organic cation transporter
Pgp	p-glycoprotein
PI	HIV-1 protease inhibitor
PSC833	valspodar
SLC	solute carrier
TDF	tenofovir disoproxil fumarate

O. Kis • J. A. Zastre • M. T. Hoque • R. Bendayan (✉)
Department of Pharmaceutical Sciences
Leslie Dan Faculty of Pharmacy, University of Toronto
144 College Street, Room 1001
Toronto, Ontario M5S 3M2, Canada
e-mail: r.bendayan@utoronto.ca

S. L. Walmsley
Faculty of Medicine, University of Toronto, Toronto, Ontario, Canada

S. L. Walmsley
Division of Infectious Diseases, University Health Network
Toronto, Ontario, Canada

Present Address:
J. A. Zastre
Department of Pharmaceutical and Biomedical Sciences
College of Pharmacy, University of Georgia
Athens, Georgia, USA

INTRODUCTION

Atazanavir is a human immunodeficiency virus (HIV)-1 protease inhibitor (PI) currently recommended in first-line regimens for treatment-naïve HIV-infected patients as well as switch regimens for patients with intolerances to other antiretroviral drugs (ARVs) (1). In first-line regimens, atazanavir is administered in combination with two nucleoside/nucleotide reverse transcriptase inhibitors (NRTIs), tenofovir disoproxil fumarate (TDF) and emtricitabine, i.e., dual-NRTI backbone. In addition, another PI, ritonavir, is recommended with atazanavir-containing regimens to improve its poor bioavailability by inhibiting atazanavir metabolic clearance by cytochrome P450 (CYP) enzymes (2). Oral bioavailability of atazanavir is also variable between patients and appears to be dependent on food intake and gastrointestinal pH (1,3,4), suggesting that intestinal absorption of atazanavir may be an important determinant of its oral bioavailability and plasma pharmacokinetics.

Intestinal epithelial cells (i.e., enterocytes) form a tight epithelial monolayer restricting paracellular entry of drugs. In addition, enterocytes are known to express several drug-metabolizing enzymes (e.g., CYPs) as well as several families of membrane-associated drug transporters, collectively acting as a biochemical barrier to drug absorption (5). ATP-binding cassette (ABC) transporters, i.e., P-glycoprotein (Pgp/MDR1), multidrug resistance-associated proteins (MRPs), and breast cancer resistance protein (BCRP) as well as solute carrier (SLC) transporters, i.e., organic anion transporting polypeptides (OATPs), organic cation transporters (OCTs), and organic anion transporters (OATs), can either facilitate or restrict drug permeability across the intestinal epithelium depending on their basolateral or apical membrane localization in enterocytes and the direction of transport (6). Drug transporters localized at the apical (brush-border) membrane, such as Pgp, MRP2, BCRP, OATPs, and OCTs, are in contact with high concentrations of drugs passing through the gastrointestinal tract and hence may be susceptible to inhibition by other co-administered drugs potentially contributing to clinical drug-drug interactions at the level of intestinal mucosa (7).

The role of CYP enzymes, such as CYP3A4, in the first-pass clearance of PIs during intestinal absorption has been demonstrated in many *in vitro* and *in vivo* studies (8). In contrast, although many *in vitro* studies identify atazanavir as a substrate for several drug transporters, the role of these transporters in the intestinal absorption and oral bioavailability of atazanavir has not been elucidated (6). *In vitro*, most PIs are substrates for Pgp (6) and *in vivo*, nelfinavir, saquinavir, and indinavir were found to have significantly higher brain accumulation in Pgp-deficient mice (Mdr1a/b-knockouts) compared to the wild-type controls (up to 40-fold higher for nelfinavir). Systemic bioavailability of these PIs was also 2–5-fold higher in Mdr1a/b-knockouts, suggesting that Pgp plays an important role in limiting oral bioavailability and tissue distribution of these PIs (9). Pgp-mediated transport is also susceptible to inhibition by many PIs, NRTIs, and NNRTIs and could potentially result in drug-drug interactions when these drugs are administered together (10–13). However, the role of Pgp in atazanavir intestinal absorption and/or drug-drug interactions remains controversial (14,15). Similarly to Pgp, MRPs are capable of transporting PIs such as atazanavir, ritonavir, lopinavir, and saquinavir (15–18) and are susceptible to inhibition by several NRTIs, such as abacavir, emtricitabine, lamivudine, and tenofovir (the parent drug form of TDF) (19). In contrast, PIs (atazanavir, ritonavir, saquinavir, lopinavir, nelfinavir) are not transported by BCRP but can potently inhibit this transporter (20,21).

Among the SLC transporters expressed in the small intestine, OATPs are believed to be the main uptake systems for poorly permeable organic anions, while organic cations are generally transported by OCTs (22,23). PIs, such as saquinavir, lopinavir, and darunavir, serve as substrates for human OATP1A2 and OATP1B1, and most PIs also inhibit OATP2B1, OATP1A2, OATP1B1, and OATP1B3 transporters (24–26). Furthermore, atazanavir intracellular accumulation by peripheral blood mononuclear cells is susceptible to inhibition by OATP family inhibitors (27). Although collectively these studies suggest that both efflux and uptake transporters may be implicated in atazanavir intestinal absorption, to date the role of drug transporters in atazanavir intestinal permeability and drug-drug interactions has not been established.

Clinical use of atazanavir is associated with many drug-drug interactions involving co-administered ARVs, some of which may involve drug transport rather than drug metabolism. For example, clinical studies report a bidirectional pharmacokinetic interaction between atazanavir and TDF. Atazanavir based regimens significantly increase plasma concentrations of tenofovir by 24–37%, while AUC and minimum plasma concentration (C_{min}) of unboosted atazanavir decrease by 25% and 23–40%, respectively, in combination with TDF (28). Because NRTIs such as TDF do not interfere with CYP-mediated metabolism of PIs, other pathways are expected to play a significant role in these interactions (6).

The aim of this study was to examine the role of intestinal ABC and SLC drug transporters in regulating atazanavir intestinal permeability and drug-drug interactions. Intestinal absorption of atazanavir was evaluated using the *in vitro* Caco-2 cell model of human intestinal epithelium and the *in situ* single-pass perfusion of rat intestine. We found that the efflux transporter Pgp can significantly restrict atazanavir permeability across Caco-2 monolayers as well as in rodent intestinal tissue segments. Furthermore, several PIs (e.g., ritonavir, darunavir,

saquinavir) and NRTIs (e.g., TDF) significantly inhibited atazanavir transport in Caco-2 cells at clinically relevant concentrations. *In situ* intestinal permeability of atazanavir was also significantly reduced in the presence of TDF, comparable to the effect observed clinically.

MATERIALS AND METHODS

Materials

^{3}H-Atazanavir (3 Ci/mmol) and ^{14}C-D-mannitol (55 mCi/mmol) were purchased from Moravek Biochemicals (Brea, CA). 6-[(2S,4R,6E)-4-Methyl-2-(methylamino)-3-oxo-6-octenoic acid]-7-L-valine-cyclosporin A, i.e., valspodar (PSC833) was a generous gift from Novartis Pharma (Basel, Switzerland). N-(4-[2-(1,2,3,4-Tetrahydro-6,7-dimethoxy-2-isoquinolinyl)ethyl]-phenyl)-9,10-dihydro-5-methoxy-9-oxo-4-acridine carboxamide (GF120918, elacridar) was a generous gift from GlaxoSmithKline Inc. (Mississauga, Canada). Fumitremorgin C was a kind gift from the laboratory of Dr. Susan Bates (Bethesda, Maryland, USA). 3-[[[3-[(1E)-2-(7-Chloro-2-quinolinyl) ethenyl]phenyl][[3-(dimethylamino)-3-oxopropyl] thio]methyl]thio]propanoic acid (MK571) was purchased from Tocris Biosciences (Ellisville, MO). Other chemicals: 3,3′-(4,5,6,7-tetrabromo-3-oxo-1(3H)-isobenzofuranylidene)-bis[6-hydroxy-benzenesulfonic acid] disodium salt (bromosulfophthalein), rifamycin SV (generic name: rifampin), pravastatin, 3-hydroxyestra-3,5(10)-trien-17-one hydrogen sulfate (i.e., estrone-3-sulfate), *p*-(dipropylsulfamoyl)benzoic acid (probenecid), *p*-aminohippurate, 4-amino-N-(2-diethylaminoethyl)benzamide hydrochloride (procainamide), 1-methyl-4-phenylpyridinium (MPP), and tetraethylammonium, were purchased from Sigma-Aldrich (Oakville, ON, Canada). Unlabeled ARVs were obtained from the National Institutes of Health AIDS research and reference reagent program, Division of AIDS (DAIDS), National Institute of Allergy and Infectious Diseases, National Institutes of Health (Bethesda, MD). Tissue culture reagents were obtained from Invitrogen (Grand Island, NY, USA), unless indicated otherwise. All buffers and Triton-X100 were purchased from Sigma-Aldrich (Oakville, ON, Canada).

Cell Culture

Caco-2 cells obtained from American Type Culture Collection (Manassas, VA) were grown in high-glucose (4.5 g/L) Dulbecco's Modified Eagle's Medium, supplemented with 10% fetal bovine serum, 2 mM L-glutamine, 1% minimal essential medium non-essential amino acids, 1% penicillin/streptomycin. Cells were maintained at 37°C in humidified 5% CO_2, with fresh medium replaced every 2–3 days, and subcultured with 0.05% trypsin-EDTA upon reaching 95% confluence. For transport experiments, Caco-2 cells were seeded at 6×10^4 cells/cm^2 cell density in 48-well plates (for drug accumulation studies) or 12-well Transwell™ polyester membrane inserts (Corning Inc., Lowell, MA), with 0.4 μM pore size and 1.12 cm^2 surface area (for drug permeability studies), and cultured for 20–23 days before use in order to achieve jejunum-like epithelial cell differentiation (29). The medium in all 48-well plates and Transwells was replaced every 2–3 days.

Transport Experiments in Caco-2 Cells

All transport experiments were performed using Hanks' balanced salt solution, containing 1.3 mM $CaCl_2$, 0.49 mM $MgCl_2$, 0.41 mM $MgSO_4$, 5.3 mM KCl, 0.44 mM KH_2PO_4, 138 mM NaCl, 0.34 mM Na_2HPO_4, and 5.6 mM D-glucose. The buffer was supplemented with 25 mM HEPES, buffered to pH 7.4, and 0.01% bovine serum albumin to reduce the binding of radiolabeled compounds to glass and plastic surfaces. Throughout this work, this HBSS buffer is referred to as transport buffer. Confluent monolayers of Caco-2 cells were preincubated with transport buffer (pH 7.4) at 37°C for 15 min, and then incubated with a similar buffer containing 0.1 μCi/ml ^{3}H-atazanavir supplemented with unlabeled atazanavir to reach the desired concentration. To evaluate the effect of an inhibitor, a specific concentration of the inhibitor was added to the preincubation buffer and the radioactive transport buffer. The inhibitors selected for the initial screening included: PSC833, a non-immunosuppressive cyclosporine A analog and a potent inhibitor of Pgp; GF120918, an acridonecarboxamide derivative and a potent inhibitor of Pgp and BCRP; fumitremorgin C, a diketopiperazine fungal toxin and a strong and specific inhibitor of BCRP; bromosulfophthalein, a dye used to assess liver function and a potent inhibitor of MRPs, OATPs, and OATs; MK571, a leukotriene D4 analog, cysteinyl leukotriene-1 receptor antagonist, and an inhibitor of most MRPs and OATPs; rifamycin SV, an antimicrobial agent and an inhibitor of OATPs and MRPs; pravastatin, a statin drug used to lower blood cholesterol and an inhibitor of OATPs, OATs, and MRPs; estrone-3-sulfate, a major precursor of biologically active estrogen and an inhibitor of OATPs, OATs, and MRPs; probenecid, a uricosuric drug that increases uric acid excretion in the urine and an inhibitor of OATPs and OATs; *p*-aminohippurate, a derivative of hippuric acid used to assess kidney function and a specific inhibitor of OATs; and three specific inhibitors of OCTs, procainamide, an antiarrhythmic agent, MPP, a neurotoxic pyridinium cation, and TEA, a quaternary ammonium cation. At the desired time interval, the radioactive medium was removed and cells were washed twice with ice-cold PBS and solubilised in 1% Triton X 100 at 37°C for 30 min. The content of each well was collected, mixed with 2 ml of PicoFluor 40

scintillation fluid (PerkinElmer, Boston, MA) and the total radioactivity was measured using a Beckman Coulter LS6500 Scintillation counter. In each experiment, "zero time" uptake was determined to correct for the non-specific binding and variable quench time, estimated by the retention of radiolabeled compound in the cells after a minimum (zero) time of exposure, determined by removing the radiolabeled solution immediately after its introduction into the well, followed by two washes with ice cold PBS and collection of cells for liquid scintillation counting. Uptake of the radiolabeled probes was normalized to total cellular protein content per well, which was measured in each well using the BioRad DC Protein Assay kit (Bio-Rad, Mississauga, Ontario, Canada) using bovine serum albumin as the standard. To evaluate inhibitory potencies of selected inhibitors and ARVs, cellular accumulation of ^{3}H-atazanavir was evaluated in the absence (DMSO or methanol control) or presence of increasing concentrations of inhibitor [I] and half maximal inhibitory concentration (IC_{50}) values were estimated by fitting the data to a sigmoidal equation (Eq. 1).

For drug permeability studies, Caco-2 cells were grown on Transwell membrane inserts at 6×10^{4} cells/cm^{2} initial seeding density and were allowed to grow for 20–23 days to achieve full differentiation of the confluent monolayer. Prior to initiating the transport studies, the transepithelial electrical resistance across the Caco-2 monolayers grown in Transwells was measured to determine the formation of a tight, uniform, and confluent monolayer with transepithelial electrical resistance values of 500–700 $\Omega \cdot \mathrm{cm}^{2}$ (29). A solution of ^{3}H-atazanavir was prepared in pH 7.4 transport buffer containing Hank's Balanced Salt Solution supplemented with 25 mM HEPES and 0.01% bovine serum albumin (to avoid the adherence of drugs or inhibitors to the plastic wells). Following 20 min pre-incubation with the inhibiting drug, the radiolabeled drug was introduced into the donor compartment (apical or basolateral) and its appearance was measured over time in the receiver compartment (basolateral or apical, respectively) by liquid scintillation counting, which allowed the estimation of the apparent permeability coefficients (P_{app}) (Eq. 2). ^{3}H-Atazanavir flux measured in apical-to-basolateral and basolateral-to-apical direction was then used to calculate the efflux ratio $\left(ER = P_{app(B-A)}/P_{app(A-B)}\right)$ (Eq. 3). Efflux ratios demonstrate the importance of active transport in restricting ($ER > 1$) or facilitating ($ER < 1$) intestinal drug absorption. To evaluate the effect of standard transporter inhibitors and drugs on atazanavir intestinal permeability, the apical-to-basolateral and basolateral-to-apical flux of atazanavir was measured in the absence or presence of specific transporter inhibitors and ARVs, which were added to the receiver and donor compartments during preincubation and transport assay.

In Situ Single-Pass Perfusion of Rat Intestine

Open-loop *in situ* single-pass perfusion studies in rat were carried out in accordance with the study protocol approved by the University of Toronto Animal Ethics Committee. The animals were housed and handled according to the University of Toronto Department of Comparative Medicine guidelines. The method was adapted from previously published protocols with some modifications (30–32). Briefly, male Sprague–Dawley rats, 300–350 g in weight, were obtained from Charles River Laboratories (Wilmington, MA) and allowed to acclimatize for 7 days. Prior to experimentation, animals were fasted overnight (12–16 h) with free access to water. Before the surgery, rats were anaesthetized with isoflurane inhalant anaesthetic and placed on a heated surface maintained at 37°C to maintain physiological body temperature. Upon disinfection with 70% isopropyl alcohol, the abdominal cavity was opened by midline incision (3–4 cm) to expose the small intestine. The two segments of interest were identified: approximately 8 cm-long jejunum segment starting 2 cm after the ligament of Treitz and 8 cm-long ileum segment ending 1 cm before the cecum. The jejunum and ileum segments were selected because of their known importance in the absorption of drugs (32–34). Pgp expression varies along the rat intestinal tract, increasing from proximal to distal regions; however, rat jejunum and ileum have very similar expression of Pgp protein and Mdr1a/1b mRNA (35). Each segment was partially opened at each end, rinsed with warmed saline and then ligated at both ends to glass cannulas (inner diameter = 4 mm) secured in place with silk sutures. The intestine was placed back into the abdominal cavity and covered with saline-wetted gauze and Parafilm. The cannulas were connected to the inlet and outlet tubing and each intestinal segment was perfused at a constant flow rate of 0.2 ml/min using a syringe infusion pump (Harvard Apparatus syringe pump, Model 22) with a pre-incubation solution containing unlabeled atazanavir (10 μM) and D-mannitol (10 μM), a non-absorbable marker, for a 30 min period to reach the steady state. To initiate the measurement of atazanavir permeability, the perfusion buffer containing ^{3}H-atazanavir and ^{14}C-D-mannitol, supplemented with unlabeled atazanavir and D-mannitol to achieve 10 μM concentrations, was introduced into the segment (at time 0) and the perfusate exiting from each segment through outlet tubing was collected into vials in consecutive 10 min intervals (control conditions). After 1 h of perfusion, the perfusion buffer was replaced with identical ^{3}H-atazanavir (10 μM) and ^{14}C-D-mannitol (10 μM) solution also containing PSC833 (5 μM) or TDF (100 μM), and the perfusate was collected in consecutive 10 min intervals over a 60 min period. Each perfusate sample was analyzed by liquid scintillation counting (measuring ^{3}H/^{14}C radioactivity) and the ^{3}H-atazanavir

concentration measured in the perfusate was corrected with ^{14}C-D-mannitol inlet/outlet concentration ratio to account for water reabsorption (Eq. 4). The steady-state effective drug permeability (P_{eff}) value was calculated at 0–60 min (control) and 60–120 min intervals (in presence of inhibitor/drug) as described in Eq. 5.

Data Analysis

Each *in vitro* (Caco-2 cell) experiment was repeated at least three times using cells from different passages. In an individual experiment, each data point represents triplicate trials. All the *in situ* experiments were performed in at least 10 animals. Results are presented as mean ± S.E.M. Statistical analysis was performed using GraphPad Prism® (version 5.01 for Microsoft Windows, Graph Pad Software, San Diego, CA, U.S.A.). Statistical significance was assessed by applying the unpaired or paired two-tailed Student's *t*-test for unpaired or paired experimental values, or the one-way analysis of variance (ANOVA) for test of repeated measures, as appropriate. A p value < 0.05 was considered statistically significant.

The IC_{50} values were extrapolated by fitting the data to a sigmoidal equation (Eq. 1) (26):

$$V_i = \frac{V_c}{1 + ([I]/IC_{50})^n} \quad (1)$$

where V_c and V_i represent atazanavir uptake in the absence (control) or presence of inhibitor, respectively; [I] is the inhibitor concentration; and n is the Hill coefficient (the largest absolute value for the slope of the curve).

To determine atazanavir permeability across the Caco-2 monolayers grown on Transwell inserts, the data for time dependent atazanavir flux in the apical-to-basolateral or basolateral-to-apical direction was fitted into Eq. 2 (29):

$$P_{app} = \frac{\Delta Q}{\Delta t} \times \frac{1}{A \times C_o} \quad (2)$$

where P_{app} is the apparent permeability coefficient (cm/s); $\Delta Q/\Delta t$ is the rate of solute flux (mol/s) from donor into the receiver compartment at steady state; A is the surface area of the filter insert (cm^2) and C_o is the initial solute concentration (mol/cm^3) in the donor compartment.

To evaluate the role of active transport in atazanavir directional permeability, the efflux ratio defined as the quotient of the secretory permeability and the absorptive permeability was determined according to Eq. 3 (29):

$$ER = \frac{P_{app(B-A)}}{P_{app(A-B)}} \quad (3)$$

where ER is the efflux ratio; $P_{app\ (A-B)}$ is the apparent permeability coefficient measured for drug permeability in the apical-to-basolateral by introducing drug into the donor compartment (apical) and measuring its appearance in the receiver compartment (basolateral); in the $P_{app\ (B-A)}$ measured in the apparent permeability coefficient measured in the basolateral-to-apical by introducing the drug into the donor compartment (basolateral) and measuring its appearance in the receiver compartment (apical).

When evaluating atazanavir intestinal permeability by *in situ* single-pass perfusion of rat intestine, the concentration of atazanavir in the perfusate exiting each segment was corrected for water reabsorption according to the Eq. 4 (33):

$$C_{out} = C_{out}(exp) \times \frac{C_{in}(D-mannitol)}{C_{out}(D-mannitol)} \quad (4)$$

where C_{out} (exp) is the experimental outlet concentration of atazanavir measured by liquid scintillation counting; C_{out} is the outlet concentration of atazanavir corrected for water reabsorption, C_{in} (D-mannitol) and C_{out} (D-mannitol) are the inlet and outlet concentrations of D-mannitol measured experimentally. The corrected outlet concentration of atazanavir was then used to determine the effective perfusion coefficient for atazanavir permeability across the rat intestinal segment at steady state (P_{eff}) according to Eq. 5 (33):

$$P_{eff} = \frac{-Q \ln(C_{out}/C_{in})}{2 \pi R L} \quad (5)$$

where Q is the flow rate (0.2 ml/min, converted to cm^3/s), C_{out}/C_{in} is the ratio of the outlet atazanavir concentration (corrected for water reabsorption) and the inlet atazanavir concentration in the perfusion buffer (i.e., 10 μM), R is the radius of rat intestine (0.18 cm) and L is the length of the intestinal segment measured after completion of perfusion (approximately 8 cm).

Data fitting into each model was performed by nonlinear least-squares analysis using GraphPad Prism® (version 5.01 for Microsoft Windows, Graph Pad Software, San Diego, CA, U.S.A.).

RESULTS

Effect of Standard Transporter Inhibitors on Atazanavir Accumulation or Uptake by Caco-2 Cells

In order to identify the transport systems implicated in atazanavir intestinal uptake or efflux, we have performed an initial screening investigating the effect of several standard inhibitors of drug efflux and uptake transporters on atazanavir accumulation by Caco-2 cells. The gene and protein expression of several ABC and SLC transporters of interest was confirmed by real-time qPCR and immunoblotting, respectively (data not shown). In the initial screening, as summarized in Table I, the

efflux of atazanavir by Caco-2 cells was highly susceptible to inhibition by Pgp inhibitors, PSC833 (1 μM) and GF120918 (5 μM), both of which increased atazanavir accumulation by more than 200%. In addition, the uptake of atazanavir into the Caco-2 cells was significantly decreased (30–50%) by the OATP family inhibitors (i.e., MK571, rifamycin SV, estrone-3-sulfate, pravastatin, and probenecid), but was unaffected by OATs inhibitor (i.e., *p*-aminohippurate) or OCTs inhibitors (i.e., procainamide, MPP, and tetraethylammonium). Although the OATP family inhibitors used in this study (i.e., MK571, rifamycin SV, estrone-3-sulfate, pravastatin, and probenecid) are also known to inhibit MRP-mediated transport and atazanavir has been reported to be a week substrate for several MRPs, in our *in vitro* studies these compounds did not inhibit atazanavir efflux by Caco-2 cells. Likewise, the BCRP inhibitor (i.e., fumitremorgin C) did not increase atazanavir accumulation by Caco-2 cells, suggesting that BCRP does not mediate atazanavir intestinal transport.

To further examine the role of Pgp and OATP family transporters in atazanavir intestinal absorption, the concentration-depended effect of these inhibitors on atazanavir accumulation was examined. Pgp inhibitors potently increased atazanavir accumulation in concentration-dependent manner, with low IC_{50} concentrations observed for both inhibitors, PSC833 (0.07 μM) and GF120918 (0.08 μM) (Fig. 1a). Five OATP family inhibitors demonstrated a concentration-dependent inhibitory effect on atazanavir uptake (measured at 10 min), with relatively high inhibitory potencies (low IC_{50} values) observed for most compounds: probenecid (3.8 μM) > estrone-3-sulfate (4.8 μM) > MK571 (5.3 μM) > rifamycin SV (17.8 μM) >>> pravastatin (4.3 mM) (Fig. 1b).

Effect of ARVs on Atazanavir Accumulation by Caco-2 Cells

In the initial screening (Table I), a number of ARVs altered atazanavir accumulation by Caco-2 cells. Some PIs, such as darunavir, lopinavir, saquinavir, and nelfinavir, significantly increased atazanavir accumulation by 40–90%. Amprenavir and tipranavir moderately but significantly decreased atazanavir accumulation, while ritonavir did not show a significant interaction with atazanavir net accumulation. Similarly, NRTIs (emtricitabine, abacavir, and lamivudine), raltegravir, and maraviroc did not significantly change atazanavir accumulation by Caco-2 cells at the concentrations tested, whereas TDF showed no interaction at 1 mM concentration, but inhibited atazanavir uptake at 100 μM concentration. To further explore the nature of these drug-drug interactions, the concentration-dependent effect of selected compounds on atazanavir accumulation by Caco-2 cells was evaluated over a range of concentrations clinically relevant with respect to the drug levels achieved in the intestine. TDF demonstrated a two-phase interaction, inhibiting atazanavir uptake into the cell at lower concentrations (0.01–100 μM), while inhibiting its efflux at higher concentrations (150–1,000 μM) (Fig. 2a). In contrast, tenofovir or emtricitabine did not alter atazanavir accumulation by Caco-2 cells (Fig. 2b and c). Several PIs inhibited atazanavir efflux from Caco-2 cells with varying potency of inhibition: saquinavir > nelfinavir > lopinavir > darunavir (Fig. 3a); however, due to the limitations in solubility of these PIs, the full concentration-dependent response curve could not be determined. Ritonavir, amprenavir, and tipranavir appeared to inhibit atazanavir cellular uptake by 25% at concentrations below 1 μM and also

Table I Effect of Standard Transporter Inhibitors and ARVs on the Accumulation or Uptake of Atazanavir by Caco-2 Cell Monolayers

Transporter inhibitor (concentration)	Accumulation of atazanavir (% control)	Antiretroviral drugs (concentration)	Accumulation of atazanavir (% control)
Control	100 ± 6.1	Control	100 ± 7.3
PSC833 (1 μM)	350 ± 27***	Ritonavir (10 μM)	89 ± 4.6
GF120918 (5 μM)	330 ± 22***	Darunavir (100 μM)	140 ± 4.9**
Fumitremorgin C (25 μM)	120 ± 13	Lopinavir (10 μM)	160 ± 11**
Bromosulfophthalein (100 μM)	98 ± 18	Saquinavir (10 μM)	190 ± 5.5***
MK571 (5 μM)	69 ± 5.0**	Amprenavir (10 μM)	67 ± 6.7**
Rifamycin SV (50 μM)	61 ± 7.1**	Tipranavir (10 μM)	80 ± 8.4*
Estrone-3-sulfate (50 μM)	65 ± 13*	Nelfinavir (10 μM)	160 ± 15**
Pravastatin (5 mM)	67 ± 6**	Tenofovir disoproxil fumarate (1 mM)	110 ± 7.8
Probenecid (500 μM)	53 ± 4.9***	Tenofovir disoproxil fumarate (100 μM)	73 ± 4.6*
p-Aminohippurate (500 μM)	90 ± 8.7	Emtricitabine (1 mM)	86 ± 7.2
Procainamide (500 μM)	93 ± 6.7	Abacavir (1 mM)	87 ± 8.1
MPP (500 μM)	98 ± 5.7	Lamivudine (1 mM)	91 ± 10
Tetraethylammonium (500 μM)	104 ± 7.5	Raltegravir (10 μM)	96 ± 9.9
		Maraviroc (10 μM)	85 ± 12

* $p < 0.05$, ** $p < 0.01$, *** $p < 0.001$

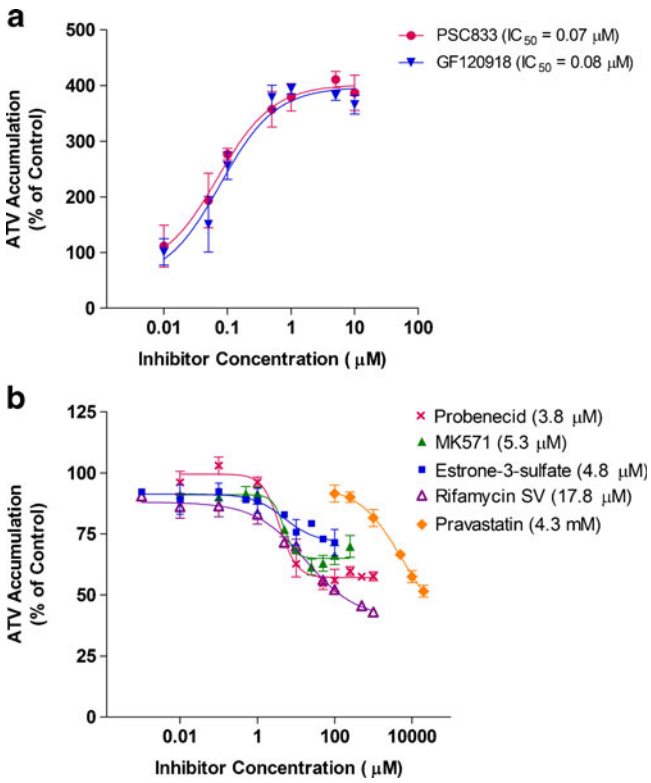

Fig. 1 Effect of Pgp and OATP family inhibitors on atazanavir (ATV) accumulation/uptake by Caco-2 monolayer cells. Cellular accumulation of ^{3}H-atazanavir (1 μM) by Caco-2 cells was measured after 60 min at pH 7.4 and 37°C in the absence (control) or presence of increasing concentrations of known Pgp inhibitors, i.e., PSC833 or GF120918 (**a**) or uptake after 10 min at pH 7.4 and 37°C in the absence (control) or presence of increasing concentrations of OATP family inhibitors, i.e., probenecid, MK571, estrone-3-sulfate, rifamycin SV, or pravastatin (**b**). The IC_{50} concentrations were determined by fitting the data into the Eq. 1 described in Materials and Methods using the GraphPad Prism 5 software. Atazanavir intracellular concentrations measured by liquid scintillation counting were normalized per mg protein and converted to percentage of DMSO control (accumulation in the absence of inhibitors). Data represent mean ± S.E.M. of at least three independent experiments.

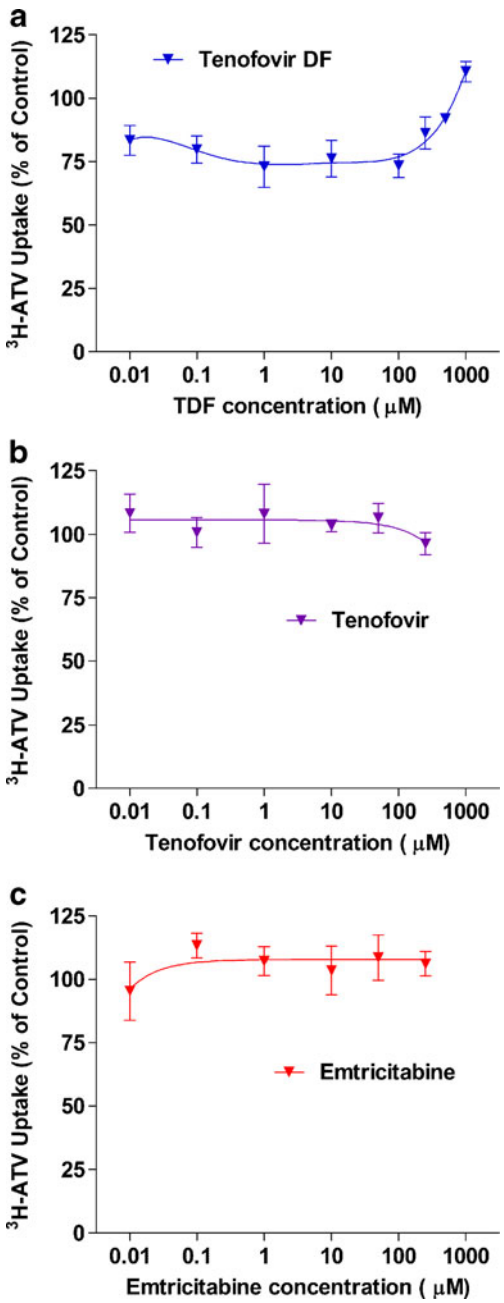

Fig. 2 Effect of NRTIs on atazanavir (ATV) accumulation by Caco-2 monolayer cells. Accumulation of ^{3}H-atazanavir (1 μM) by Caco-2 cells was measured after 60 min at pH 7.4 and 37°C in the absence (control) or presence of increasing concentrations of TDF (**a**), tenofovir (**b**), or emtricitabine (**c**). Atazanavir intracellular concentrations measured by liquid scintillation counting were normalized per mg protein and converted to percentage of DMSO (for TDF) or water (for tenofovir and emtricitabine) control. Data represent mean ± S.E.M. of at least three independent experiments.

demonstrated efflux inhibition at higher concentrations (Fig. 3b), which explained the apparent lack of interaction observed for ritonavir in the initial screening (Table I). When Pgp-mediated transport was inhibited with PSC833 (1 μM), concentration-dependent inhibition of atazanavir uptake by these PIs was observed, with low IC_{50} values for ritonavir (0.5 μM), amprenavir (1.4 μM), and tipranavir (2.1 μM) (Fig. 3c).

Atazanavir Permeability Across Caco-2 Monolayers

In order to examine the role of drug transport in facilitating or restricting atazanavir intestinal permeability and bioavailability, we evaluated *in vitro* atazanavir flux across Caco-2 monolayers grown on Transwell microporous filter membranes to model human intestinal epithelium. Membrane localization of Pgp in fully differentiated Caco-2 cell monolayers grown on Transwell inserts was examined by immunocytochemical analysis, applying laser confocal microscopy, which confirmed that Pgp is localized exclusively at the apical membrane of Caco-2 cells (data not shown). In the absence of inhibitors, the permeability of

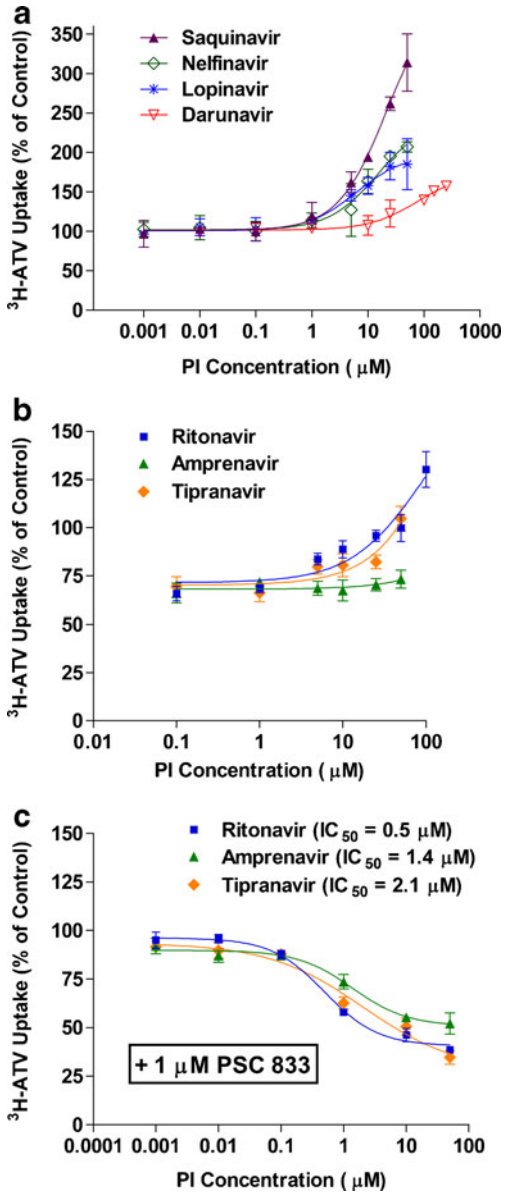

Fig. 3 Effect of PIs on atazanavir (ATV) accumulation by Caco-2 monolayer cells. Accumulation of ^{3}H-atazanavir (1 μM) by Caco-2 cells was measured after 60 min at pH 7.4 and 37°C in the absence (control) or presence of increasing concentrations of saquinavir, nelfinavir, lopinavir or darunavir (**a**) or ritonavir, tipranavir or amprenavir examined in the absence (**b**) or presence of 1 μM PSC833 (**c**). The IC_{50} concentrations were determined by fitting the data into the Eq. 1 using the GraphPad Prism 5 software. Atazanavir intracellular concentrations measured by liquid scintillation counting were normalized per mg protein and converted to percentage of DMSO control (accumulation in the absence of inhibitors). Data represent mean ± S.E.M. of at least three independent experiments.

atazanavir (1 μM) in the apical-to-basolateral direction ($P_{app(A-B)}$) was significantly lower from that measured in the basolateral-to-apical direction ($P_{app(B-A)}$) (Fig. 4a), with a high efflux ratio ($P_{app(B-A)}/P_{app(A-B)}$) above 10. With increasing atazanavir concentrations, the ratio of atazanavir basolateral-to-apical and apical-to-basolateral P_{app} gradually decreased, approaching an efflux ratio of 1 at 100 μM concentration, indicating a saturable effect. Addition of Pgp inhibitor (i.e., 1 μM PSC833) resulted in increased apical-to-basolateral flux and decreased basolateral-to-apical atazanavir flux (Fig. 4b) with efflux ratios approaching 1 at all atazanavir concentrations (1–100 μM) (Fig. 4c) and a similar effect was observed with GF120918 (5 μM) (Table II), demonstrating that atazanavir efflux at the apical membrane of Caco-2 cells is Pgp-mediated. Ritonavir, a potent inhibitor of Pgp, exerted a very similar effect, significantly increasing apical-to-basolateral flux and decreasing basolateral-to-apical flux of atazanavir, resulting in a net decrease in the efflux ratio of atazanavir from 11.7 to 1.7. Hence, while ritonavir can inhibit both uptake and efflux of atazanavir during intracellular accumulation assays in Caco-2 cells grown on solid support, when examining the vectorial transport of atazanavir across Caco-2 monolayers, ritonavir primarily inhibits the Pgp-mediated efflux of atazanavir at the apical membrane resulting in reduction in its efflux ratio. Other ARVs known to interact with Pgp (i.e., TDF, emtricitabine, maraviroc, darunavir, and amprenavir) also demonstrated a significant although less potent reduction in atazanavir efflux ratio (Table II).

Effect of Pgp Inhibitor on Atazanavir *In Situ* Intestinal Permeability in Rat Intestinal Segments

The effect of Pgp inhibitor, PSC833, on atazanavir intestinal absorption was examined applying an *in situ* single-pass intestinal perfusion technique in Sprague–Dawley rats. Steady-state permeability of 10 μM atazanavir in the proximal jejunum (Fig. 5a) and distal ileum (Fig. 5b) segments of rat intestine was measured over a two-hour period. These segments were selected because of their known importance in the absorption of drugs (32–34). In each animal, atazanavir permeability (P_{eff}) during the first hour (0–60 min) in the absence of inhibitor (control) was compared to P_{eff} obtained in the same animal during the second hour, when 5 μM PSC833 was present in the perfusate buffer (60–120 min), in order to use each animal as its own control. A control experiment was also conducted, measuring atazanavir P_{eff} in the absence of inhibition during both periods or in the presence of 5 μM PSC833 during both perfusion periods, repeated in three rats per group (data not shown). In these control experiments, no significant difference was observed between atazanavir permeability during the 0–60 min period and the 60–120 min period when the experimental conditions were maintained the same. Paired statistical analysis (paired Student's *t*-test) of P_{eff} values obtained in the absence (control) and presence of PSC833 in each animal was performed for 10 animals. Pgp inhibition increased atazanavir permeability (P_{eff}) in the jejunum from $2.8 \pm 1.1 \times 10^{-5}$ cm/s to $4.8 \pm 1.4 \times 10^{-5}$ cm/s, corresponding to a decrease in atazanavir steady-

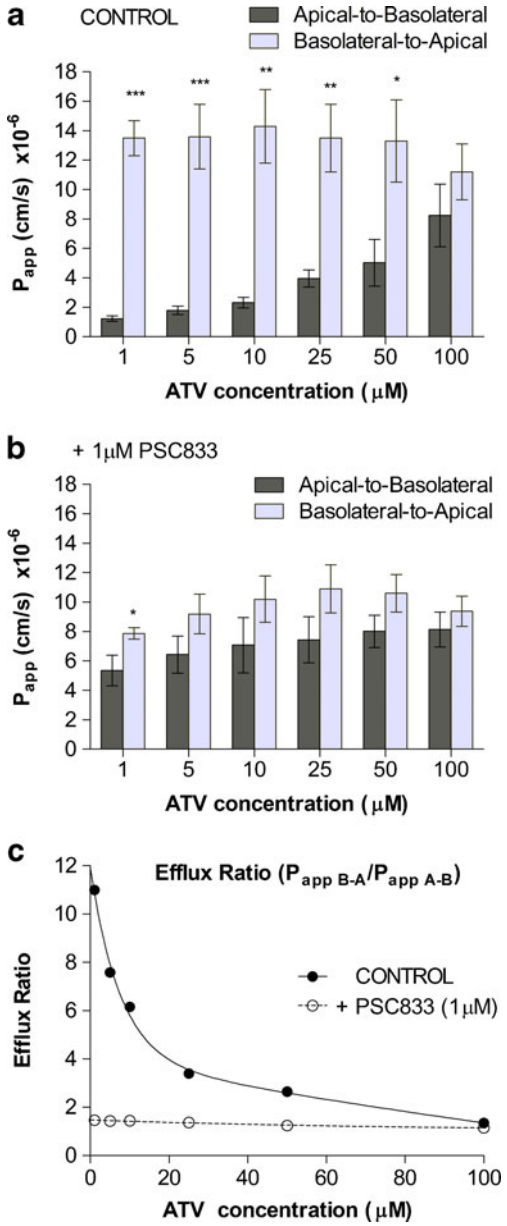

Fig. 4 Concentration dependence of atazanavir (ATV) intestinal permeability across Caco-2 monolayer cells in the apical-to-basolateral and basolateral-to-apical directions. The flux of atazanavir in the apical-to-basolateral or basolateral-to-apical direction was determined by introducing ^{3}H-atazanavir (1–100 μM) into the donor compartment and measuring its appearance over time in the receiver compartment in the absence (**a**) or presence of 1 μM PSC833 (**b**) to calculate the apparent permeability coefficients (P_{app}) according to Eq. 2. Efflux ratio ($ER = P_{app(B-A)}/P_{app(A-B)}$) was then calculated for atazanavir permeability at different concentrations in the absence or presence of 1 μM PSC833 according to Eq. 3, as described in Materials and Methods, and plotted against the atazanavir concentration (**c**). Data represent mean ± S.E.M. of at least three independent experiments. * $p<0.05$, ** $p<0.01$, *** $p<0.001$.

state C_{out} concentration in the perfusate from 9.24±0.25 μM to 8.72±0.32 μM. Similarly, in the ileum atazanavir P_{eff} increased from $2.4\pm0.7\times10^{-5}$ cm/s to $4.1\pm0.9\times10^{-5}$ cm/s, corresponding to reduction in C_{out} from 9.33±0.18 μM to 8.87±0.20 μM. Paired data analysis comparing atazanavir steady-state P_{eff} before and after the addition of PSC833 in each animal demonstrated significant increases in atazanavir permeability both in the jejunum (average increase of 78% [47–153%], $p<0.0001$) and ileum (average increase of 79% [46% to 127%], $p<0.0001$).

Interactions Between Atazanavir and TDF in the *In Situ* Single-Pass Rodent Intestinal Perfusion Model

In order to further examine the role of the intestinal epithelium in clinical drug-drug interactions between atazanavir and TDF, we investigated the effect of TDF on the steady-state intestinal permeability of atazanavir *in situ*. Since TDF prodrug is known to have poor water solubility compared to other NRTIs, 100 μM concentration of TDF was selected for the *in situ* single-pass perfusion studies in Sprague–Dawley rats. The flux of 10 μM ^{3}H-atazanavir across the jejunum (Fig. 6a) and ileum (Fig. 6b) segments in each animal was evaluated in the absence (control, 0–60 min interval) or presence of 100 μM TDF (60–120 min interval). In each animal, steady-state atazanavir P_{eff} was measured in the absence (control) or presence of TDF, using each animal as its own control. Paired statistical analysis (paired Student's *t*-test) of data obtained from 10 animals was used to determine significant changes in atazanavir permeability due to TDF. Following the co-administration of 100 μM TDF in the second interval (60–120 min), atazanavir steady-state P_{eff} decreased on average 25% [13–40%] ($p<0.0001$) in the jejunum, with an observed increase in C_{out} from 9.24±0.24 μM to 9.43±0.19 μM. Similarly, in the ileum the P_{eff} decreased 28% [16% to 49%] ($p=0.0002$), with an observed increase in C_{out} from 9.39±0.16 μM to 9.57±0.11 μM.

DISCUSSION

Current HIV treatment guidelines recommend atazanavir as the preferred component of antiretroviral combination regimens for treatment-naïve and -experienced HIV-infected patients. Although atazanavir has favourable efficacy and safety profile, several challenges are associated with its clinical use, such as poor and highly variable oral bioavailability as well as a large number of drug-drug interactions. Extensive metabolism of atazanavir by CYP3A4 in the liver and intestine is a major determinant of its first-pass extraction and elimination. Furthermore, many drug-drug interactions have been attributed to changes in atazanavir metabolism by CYP3A4, including the boosting effect of ritonavir on atazanavir bioavailability. However, the role of drug transporters in atazanavir pharmacokinetics and tissue distribution remains controversial. While a number of studies report that atazanavir is a substrate for Pgp and MRP family transporters, as well

Table II Effect of Pgp Inhibitors and ARVs on the Apical-to-basolateral and Basolateral-to-apical Permeability of 1 μM Atazanavir Across Caco-2 Monolayer Cells

Inhibitor/drug (concentration)	Apical-to-basolateral P_{app} (cm/s) × 10^{-6}	Basolateral-to-apical P_{app} (cm/s) × 10^{-6}	Efflux ratio
Control	1.2 ± 0.19	14 ± 1.2	11.7
PSC833 (1 μM)	5.4 ± 1.0***	7.9 ± 0.39**	1.5
GF120918 (5 μM)	6.7 ± 0.91***	9.9 ± 1.5*	1.5
Ritonavir (10 μM)	5.8 ± 0.41***	9.6 ± 1.9*	1.7
Darunavir (10 μM)	2.2 ± 0.53	16 ± 0.24	7.3
Amprenavir (10 μM)	3.1 ± 0.35**	15 ± 1.5	5.0
Tenofovir disoproxil fumarate (250 μM)	3.3 ± 0.23***	10 ± 0.50*	3.0
Emtricitabine (250 μM)	2.5 ± 0.12**	10 ± 0.049**	4.0
Maraviroc (10 μM)	3.3 ± 0.71**	9.8 ± 0.10**	3.0

* $p < 0.05$, ** $p < 0.01$, *** $p < 0.001$

as an OATP-like transport system in lymphocytes (27,36,37), other studies suggest that atazanavir is a poor substrate for Pgp and MRPs (15) and that Pgp plays a minor role in atazanavir intestinal transport and drug-drug interactions with ritonavir (14). However, in our previous study we have

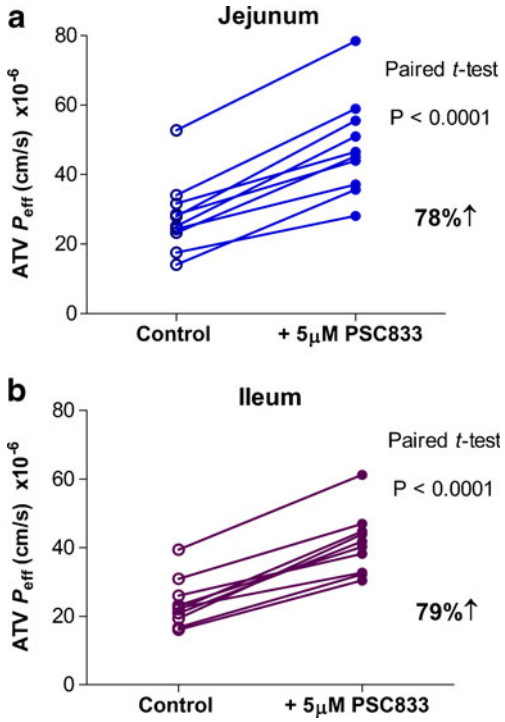

Fig. 5 Effect of Pgp inhibitor, PSC833, on atazanavir (ATV) intestinal permeability measured by *in situ* single-pass perfusion of rat intestinal segments. The effective permeability (P_{eff}) of atazanavir was measured in the jejunum (**a**) or ileum (**b**) segment of rat intestine in each animal by *in situ* single-pass perfusion, as described in Materials and Methods. The intestinal segment was perfused with 10 μM ^{3}H-atazanavir at pH 6.5 first without inhibitor (first hour, control) and then in the presence of 5 μM PSC833 (second hour). Atazanavir concentrations in the perfusate were corrected for water reabsorption according to Eq. 4. The steady-state P_{eff} values were calculated according to Eq. 5. The effect of PSC833 on atazanavir permeability was evaluated by comparing the P_{eff} values measured in the first (control) and second hour of perfusion in each animal in the jejunum and ileum segment. Paired Student's *t*-test analysis was used to determine the statistical significance of the changes in atazanavir P_{eff} in the presence of Pgp inhibitor, PSC833. The measurements were repeated in 10 Sprague–Dawley rats.

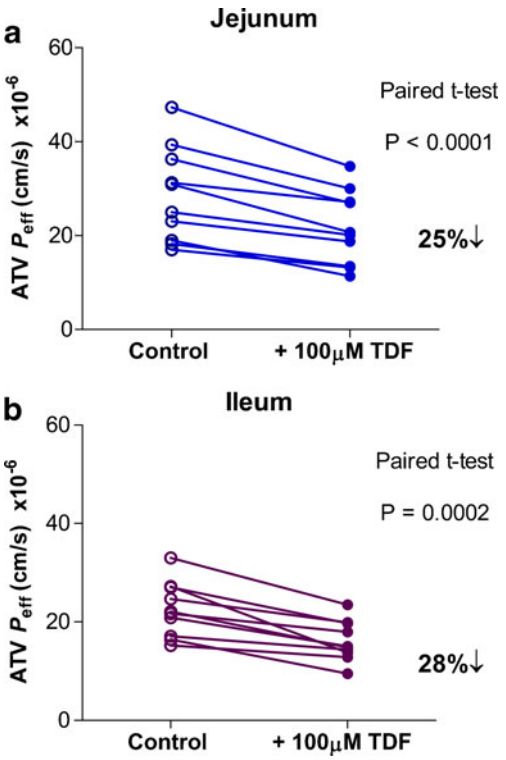

Fig. 6 Effect of TDF on atazanavir (ATV) intestinal permeability measured by *in situ* single-pass perfusion of rat intestinal segments. The effective permeability (P_{eff}) of ^{3}H-atazanavir was measured in the jejunum (**a**) or ileum (**b**) segment of the intestine in each animal by *in situ* single-pass perfusion, as described in Materials and Methods. The intestinal segment was perfused with 10 μM ^{3}H-atazanavir at pH 6.5 first without inhibitor (first hour, control) and then in the presence of 100 μM TDF (second hour). Atazanavir concentrations in the perfusate were corrected for water reabsorption according to Eq. 4. The steady-state P_{eff} values were calculated according to Eq. 5. The effect of TDF on atazanavir permeability was evaluated by comparing the P_{eff} values measured in the first (control) and second hour of perfusion in each animal in the jejunum and ileum segments. Paired Student's *t*-test analysis was used to determine the statistical significance of the changes in atazanavir P_{eff} due to the co-administration of TDF. The measurements were repeated in 10 Sprague–Dawley rats.

demonstrated that Pgp-overexpressing MDA cells have over 5-fold lower accumulation of atazanavir compared to the wild-type cells, indicating that Pgp-mediated efflux strongly restricts atazanavir intracellular accumulation (36). In addition, several studies report that Pgp plays an important role in the intestinal first-pass extraction of other PIs, such as nelfinavir, saquinavir, and indinavir, significantly limiting their oral bioavailability (6). In the present study, we provide the first evidence that Pgp and other drug transporters can regulate atazanavir intestinal absorption and in part contribute to the clinically significant drug-drug interactions of atazanavir with other ARVs, such as ritonavir and TDF.

In order to investigate the role of drug transporters in atazanavir absorption, we have utilized the Caco-2 cell line derived from human colon carcinoma cells, a well-established *in vitro* model used to predict human drug absorption and drug-drug interactions. Caco-2 cells have been extensively characterized in other studies and have been shown to express very low amounts of CYP enzymes, making this model especially suitable for examining various substrates transport properties. Furthermore, the expression of several families of drug efflux and uptake transporters in Caco-2 cells correlates well with their expression in the human jejunum (38,39). Due to the reported high variability in drug transporter expression in Caco-2 cells from different laboratories (40), we have characterized in our own hands the gene and protein expression of several drug transporters of interest in fully-differentiated Caco-2 cells which were used for transport experiments (data not shown). Furthermore, we have also confirmed apical (brush-border) membrane localization of Pgp in Caco-2 cells grown on Transwell membrane inserts by immunocytochemistry analysis (data not shown). Pgp localization at the apical membrane allows this efflux pump to restrict the absorptive permeability of substrate drugs from the lumen into the portal circulation while enhancing their secretory flux back into the lumen, leading to a net reduction in oral drug bioavailability.

To characterize the role of Pgp in atazanavir intestinal absorption, we examined the effect of Pgp inhibitors on: the *in vitro* accumulation of atazanavir by Caco-2 cells, the absorptive (apical-to-basolateral) and secretory (basolateral-to-apical) flux of atazanavir across the Caco-2 monolayers grown on Transwell membrane inserts, and the *in situ* intestinal absorption of atazanavir in rodent intestinal segments, jejunum and ileum. Atazanavir accumulation by Caco-2 cells was highly susceptible to inhibition by two established Pgp inhibitors, PSC833 and GF120918 (IC_{50} concentrations below 0.1 μM). In addition, the secretory flux of atazanavir was 11.7-fold higher than its absorptive flux, comparable to the efflux ratios reported for other Pgp substrates, such as digoxin (41). This efflux ratio was saturable with increasing concentrations of atazanavir and susceptible to inhibition by Pgp inhibitors, PSC833 and GF120918, both of which reduced the efflux ratio to 1.5. These data strongly suggest that Pgp-mediated efflux is involved in the limited absorptive permeability of atazanavir across Caco-2 cell monolayers.

Since Pgp mediates active efflux of drugs back into the lumen, we proposed that Pgp could significantly contribute to the overall intestinal permeability of atazanavir, even in the presence of CYP-mediated metabolism. To test this hypothesis, we utilized an *in situ* single-pass rodent perfusion model of drug absorption. This model offers many advantages over the *in vitro* and *ex vivo* techniques, such as the continuous blood flow to and from the perfused segment creating sink conditions, a preserved microenvironment at the mucosal membrane, and regional differences in the expression of drug transporters and metabolic enzymes along the gastrointestinal tract (42). In this model, inhibition of Pgp by PSC833 resulted in a significant increase in atazanavir steady-state permeability in both intestinal segments: 78% [47–153%] in the jejunum and 79% [46–127%] in the ileum. These data suggest that Pgp-mediated efflux also plays a significant role in limiting intestinal absorption of atazanavir. Hence, the poor oral bioavailability of atazanavir is the result of the interplay of CYP3A4-mediated metabolism within the enterocytes and Pgp-mediated efflux back into the lumen.

Although several MRPs are known to recognize atazanavir as a substrate (27,36,37), we found that MRPs play a minor role in atazanavir efflux from Caco-2 cells, while an OATP-like uptake system appears to mediate atazanavir uptake into the cell. Several MRP-family inhibitors (MK571, probenecid, rifamycin SV, estrone-3-sulfate, and pravastatin), which are also known to interact with OATP and OAT transporters, were evaluated for their ability to inhibit atazanavir transport in Caco-2 cells. Interestingly, all of these compounds reduced cellular uptake of atazanavir in a concentration-dependent manner, demonstrating inhibition of atazanavir uptake rather than efflux. These data suggest that atazanavir uptake into the cell is carrier-mediated, contrary to the previously accepted mechanism of atazanavir cellular entry by simple diffusion. Although all MRP family inhibitors used in these studies also inhibit OATPs and OATs, a more specific inhibitor of OAT family, *p*-aminohippurate, did not alter atazanavir uptake by Caco-2 cells, suggesting the involvement of an OATP-like transport system. These findings are also in agreement with a previous study reporting that atazanavir uptake by peripheral blood mononuclear cells is susceptible to inhibition by OATP family inhibitors (27). Due to the lack of specificity of OATP family inhibitors (43,44), we were not able to identify the OATP isoform(s) implicated in atazanavir uptake by Caco-2 cells or the enterocytes of the jejunum or ileum. Intestinal epithelial cells are known to express several OATP isoforms including OATP1A2, OATP2B1, OATP3A1, and

OATP4A1, as well as OATP1B1 and OATP1B3 transcripts (45–47). Previous studies indicate that atazanavir inhibits transport activity of several OATPs such as OATP2B1, OATP1B1, and OATP1B3 transporters (24,26). Furthermore, we have previously demonstrated that atazanavir is not a substrate for OATP2B1 (26); however, the role of other intestinal OATPs in atazanavir intestinal transport has not been examined to date.

Since drug transporters appear to play a significant role in atazanavir intestinal absorption, we hypothesized that the inhibition of these drug transporters by other drugs may contribute to the clinically reported drug-drug interactions involving atazanavir. In particular, several drug-drug interactions occur clinically between atazanavir and other ARVs co-administered in first-line and/or salvage HIV therapy, such as NRTIs (i.e., TDF, emtricitabine, abacavir, and lamivudine), other PIs (i.e., ritonavir, darunavir, lopinavir, saquinavir, amprenavir, tipranavir, and nelfinavir), and newer classes of antiretrovirals (i.e., raltegravir and maraviroc) (1). The maximum concentrations of drugs achieved in the intestinal lumen are much higher than their plasma concentrations, especially for drugs that have poor oral bioavailability, such as PIs and NNRTIs. Intestinal drug concentrations are generally estimated as the orally administered drug dose dissolved in 250 ml, the accepted minimal gastric volume or the volume of liquid intake with medication (33). Based on currently recommended doses (1), the maximum intestinal concentrations of ARVs can be estimated as 0.5–8 mM for PIs, 0.8–3.5 mM for NRTIs, and 1–3.5 mM for NNRTIs. These estimates, however, do not account for the solubility of these drugs, a potential limiting factor for poorly water-soluble drugs such as PIs and some other ARVs known to have poor water solubility (e.g., TDF), which may only reach 100–200 μM maximum concentrations in the aqueous solution. In contrast, highly water-soluble drugs such as most NRTIs can achieve millimolar concentrations in the intestinal lumen. In the drug-drug interaction studies performed in Caco-2 cells, we have selected the concentrations of ARVs that mimic clinically relevant intestinal concentrations of these drugs, i.e., up to 100 μM for PIs (except darunavir which has better water solubility) and up to 1 mM for NRTIs.

From previous studies, PIs are known to inhibit several families of drug transporters, in particular Pgp, MRPs, BCRP, OATPs, and OCTs (6). Since the apical membrane of the enterocytes is exposed to high drug concentrations within the intestinal lumen, we anticipated that drug transporters localized at the apical membrane (i.e., Pgp, MRP2, BCRP, and OATPs) will be the most susceptible to inhibition by other drugs and therefore may contribute to atazanavir drug-drug interactions. As expected, some PIs known to interact with Pgp inhibited atazanavir efflux from Caco-2 cells: saquinavir > nelfinavir > lopinavir > darunavir. In addition, ritonavir, amprenavir, and tipranavir appeared to inhibit both uptake and efflux of atazanavir (Fig. 3), with potent concentration-dependent inhibition of uptake (IC_{50} <2 μM) observed when Pgp activity was blocked by PSC833. These findings suggest that complex drug-drug interactions may occur between atazanavir and other PIs during oral absorption. In particular ritonavir, known for its inhibitory effect on atazanavir metabolism by CYP3A4, may also interfere with atazanavir uptake and efflux during intestinal absorption. In Caco-2 permeability assays, ritonavir co-administration resulted in nearly 5-fold increase in atazanavir absorptive flux ($p<0.001$) and decrease in atazanavir efflux ratio from 11.7 to 1.7, similarly to the effect of Pgp inhibitors PSC833 and GF120918. These findings suggest that the "boosting effect" of ritonavir on atazanavir oral bioavailability observed clinically may be due to the combined inhibition of Pgp-mediated efflux and CYP3A-mediated metabolism of atazanavir. Furthermore, in Caco-2 Transwell permeability assays, ARVs which can inhibit both uptake and efflux of atazanavir in Caco-2 cells, such as ritonavir, amprenavir, and TDF, appear to predominantly inhibit the Pgp-mediated efflux of atazanavir in the apical-to-basolateral and basolateral-to-apical vectorial transport, leading to a decrease in atazanavir efflux ratio, while uptake inhibition only affects atazanavir intracellular accumulation but not its transepithelial transport.

Among other ARVs commonly co-administered with atazanavir, TDF and emtricitabine constitute the recommended NRTI backbone. Interestingly, TDF co-administration significantly decreases the AUC and C_{min} of unboosted or boosted atazanavir by 25% and 23–40%, respectively (28). Because TDF does not interfere with CYP-mediated drug metabolism (48), drug transporters are expected to play a significant role in this drug-drug interaction. Furthermore, *in vitro* studies examining TDF permeability across Caco-2 monolayers have demonstrated that PIs increase TDF intestinal permeability in part through inhibition of Pgp-mediated efflux of TDF (49). However, the effect of TDF on the intestinal absorption of PIs such as atazanavir has not been examined to date. In the *in vitro* Caco-2 cell model, TDF demonstrated a two-phase interaction, inhibiting atazanavir uptake into the cell at lower concentrations (0.01–100 μM), while inhibiting its efflux at higher concentrations (150–1,000 μM). However, in the *in situ* model, co-administration of 100 μM TDF resulted in a significant decrease in atazanavir steady-state P_{eff} values, with an average decrease of 25% [13% to 40%] in the jejunum and 28% [16% to 49%] in the ileum. These findings are in agreement with the clinically reported effect of TDF on atazanavir pharmacokinetics and suggest that this clinical drug-drug interaction may occur during oral absorption of atazanavir. Based on previous studies, neither TDF pro-drug nor the parent drug tenofovir are substrates or inhibitors of CYP450 enzymes at

concentrations substantially higher than those observed in the clinic (50,51). Since atazanavir metabolism is primarily mediated by CYP3A enzymes (52–54), it is unlikely that the effect of TDF on atazanavir intestinal permeability *in situ* is due to the inhibition of metabolic pathways. Based on the data from *in vitro* and *in situ* studies, we propose that a potential mechanism for this interaction could involve TDF-mediated inhibition of atazanavir uptake by the OATP-like transport system at the apical membrane of enterocytes and/or inhibition of atazanavir efflux into the portal circulation by MRP isoforms at the basolateral side (i.e., MRP1, MRP3, and MRP5), which recognize atazanavir as a substrate (6,15,27,36,37). Further studies are needed to fully elucidate the mechanism of this drug-drug interaction.

CONCLUSION

Using two established models of human intestinal drug absorption, we demonstrate for the first time that Pgp plays an important role in limiting atazanavir oral bioavailability, while its uptake into the cell is carrier-mediated, with apparent involvement of an OATP uptake system. Atazanavir transport is susceptible to inhibition by other ARVs, particularly ritonavir, which strongly inhibits Pgp-mediated efflux of atazanavir *in vitro* and *in situ*. Hence, the "boosting effect" of ritonavir on atazanavir bioavailability appears to be due to the combined inhibition of CYP3A4-mediated metabolism and Pgp-mediated efflux of atazanavir in the intestine. We also observe that clinical interactions between atazanavir and TDF may occur at the intestinal mucosa and be potentially avoided by staggering the administration of these two ARVs. Further clinical studies investigating the role of intestinal drug transporters in atazanavir absorption and drug-drug interactions in human subjects are needed.

ACKNOWLEDGMENTS AND DISCLOSURES

This work is supported by the Canadian Foundation for AIDS Research [Grant 20023 awarded to RB]. Drs. Reina Bendayan and Sharon Walmsley are recipients of the Ontario HIV Treatment Network (OHTN) Career Scientist award. Ms. Olena Kis was supported by Ph.D. studentships from the OHTN, Ministry of Health of Ontario, and the National Science and Engineering Research Council of Canada (NSERC) and is currently a recipient of the Canadian Institutes of Health Research (CIHR) Frederick Banting and Charles Best—Canada Graduate Scholarship. Dr. Jason Zastre was a postdoctoral fellow in the laboratory or Dr. Reina Bendayan when this study was initiated and is currently an Assistant Professor in the Department of Pharmaceutical and Biomedical Sciences, College of Pharmacy University of Georgia, Athens, Georgia.

We thank Dr. David E. Smith (Department of Pharmaceutical Sciences, University of Michigan College of Pharmacy) for providing excellent guidance with the implementation of the rodent *in situ* single-pass perfusion technique.

REFERENCES

1. Panel on Antiretroviral Guidelines for Adults and Adolescents. Guidelines for the use of antiretroviral agents in HIV-1 infected adults and adolescents. Department of Health and Human Services; 2012 Mar 27.
2. von Hentig N. Atazanavir/ritonavir: a review of its use in HIV therapy. Drugs Today (Barc). 2008;44(2):103–32.
3. Bristol Myers Squibb Company. Princeton, NJ, USA. Reyataz product information. 2012.
4. Giguere P, Burry J, Beique L, Zhang G, Angel J, la Porte C. The effect of food on the pharmacokinetics of atazanavir/ritonavir 300/100 mg daily in HIV-infected patients. 11th International Workshop on Clinical Pharmacology and HIV Therapy. 2010 Apr 7. Report No. 30: Sorrento, Italy.
5. Bruyere A, Decleves X, Bouzom F, Ball K, Marques C, Treton X, *et al.* Effect of Variations in the Amounts of P-Glycoprotein (ABCB1), BCRP (ABCG2) and CYP3A4 along the Human Small Intestine on PBPK Models for Predicting Intestinal First Pass. Mol Pharm. 2010;7(5):1596–607.
6. Kis O, Robillard K, Chan GN, Bendayan R. The complexities of antiretroviral drug-drug interactions: role of ABC and SLC transporters. Trends Pharmacol Sci. 2010;31(1):22–35.
7. Chan LM, Lowes S, Hirst BH. The ABCs of drug transport in intestine and liver: efflux proteins limiting drug absorption and bioavailability. Eur J Pharm Sci. 2004;21(1):25–51.
8. Wynn GH, Zapor MJ, Smith BH, Wortmann G, Oesterheld JR, Armstrong SC, *et al.* Antiretrovirals, part 1: overview, history, and focus on protease inhibitors. Psychosomatics. 2004;45(3):262–70.
9. Kim RB, Fromm MF, Wandel C, Leake B, Wood AJ, Roden DM, *et al.* The drug transporter P-glycoprotein limits oral absorption and brain entry of HIV-1 protease inhibitors. J Clin Invest. 1998;101(2):289–94.
10. Storch CH, Theile D, Lindenmaier H, Haefeli WE, Weiss J. Comparison of the inhibitory activity of anti-HIV drugs on P-glycoprotein. Biochem Pharmacol. 2007;73(10):1573–81.
11. Perloff ES, Duan SX, Skolnik PR, Greenblatt DJ, von Moltke LL. Atazanavir: effects on P-glycoprotein transport and CYP3A metabolism *in vitro*. Drug Metab Dispos. 2005;33(6):764–70.
12. Perloff MD, Von Moltke LL, Fahey JM, Daily JP, Greenblatt DJ. Induction of P-glycoprotein expression by HIV protease inhibitors in cell culture. AIDS. 2000;14(9):1287–9.
13. Weiss J, Weis N, Ketabi-Kiyanvash N, Storch CH, Haefeli WE. Comparison of the induction of P-glycoprotein activity by nucleotide, nucleoside, and non-nucleoside reverse transcriptase inhibitors. Eur J Pharmacol. 2008;579(1–3):104–9.
14. Holmstock NF, Annaert PP, Augustijns P. Boosting of HIV protease inhibitors by ritonavir in the intestine: the relative role of Cyp and P-gp inhibition based on Caco-2 monolayers *versus in situ* intestinal perfusion in mice. Drug Metab Dispos. 2012;40(8):1473–7.
15. Bierman WF, Scheffer GL, Schoonderwoerd A, Jansen G, van Agtmael MA, Danner SA, *et al.* Protease inhibitors atazanavir, lopinavir and ritonavir are potent blockers, but poor substrates, of ABC transporters in a broad panel of ABC transporter-overexpressing cell lines. J Antimicrob Chemother. 2010;65(8):1672–80.
16. van der Sandt I, Vos CM, Nabulsi L, Blom-Roosemalen MC, Voorwinden HH, de Boer AG, *et al.* Assessment of active transport

of HIV protease inhibitors in various cell lines and the *in vitro* blood–brain barrier. AIDS. 2001;15(4):483–91.
17. Janneh O, Owen A, Chandler B, Hartkoorn RC, Hart CA, Bray PG, *et al.* Modulation of the intracellular accumulation of saquinavir in peripheral blood mononuclear cells by inhibitors of MRP1, MRP2, P-gp and BCRP. AIDS. 2005;19(18):2097–102.
18. Huisman MT, Smit JW, Crommentuyn KM, Zelcer N, Wiltshire HR, Beijnen JH, *et al.* Multidrug resistance protein 2 (MRP2) transports HIV protease inhibitors, and transport can be enhanced by other drugs. AIDS. 2002;16(17):2295–301.
19. Weiss J, Theile D, Ketabi-Kiyanvash N, Lindenmaier H, Haefeli WE. Inhibition of MRP1/ABCC1, MRP2/ABCC2, and MRP3/ABCC3 by nucleoside, nucleotide, and non-nucleoside reverse transcriptase inhibitors. Drug Metab Dispos. 2007;35(3):340–4.
20. Weiss J, Rose J, Storch CH, Ketabi-Kiyanvash N, Sauer A, Haefeli WE, *et al.* Modulation of human BCRP (ABCG2) activity by anti-HIV drugs. J Antimicrob Chemother. 2007;59(2):238–45.
21. Gupta A, Zhang Y, Unadkat JD, Mao Q. HIV protease inhibitors are inhibitors but not substrates of the human breast cancer resistance protein (BCRP/ABCG2). J Pharmacol Exp Ther. 2004;310(1):334–41.
22. Kim RB. Organic anion-transporting polypeptide (OATP) transporter family and drug disposition. Eur J Clin Invest. 2003;33 Suppl 2:1–5.
23. Nakamura T, Yamamori M, Sakaeda T. Pharmacogenetics of intestinal absorption. Curr Drug Deliv. 2008;5(3):153–69.
24. Annaert P, Ye ZW, Stieger B, Augustijns P. Interaction of HIV protease inhibitors with OATP1B1, 1B3, and 2B1. Xenobiotica. 2010;40(3):163–76.
25. Demby VE, Harmon KA, Naqwel M, Humphreys JE, Wire M, Polli JW. OATP1B1, OATP1B3 and BCRP transporter characterization for fosamprenavir, amprenavir and lopinavir. 2008 AAPS Annual Meeting and Exposition. 2008;2355.
26. Kis O, Zastre JA, Ramaswamy M, Bendayan R. pH dependence of organic anion-transporting polypeptide 2B1 in Caco-2 cells: potential role in antiretroviral drug oral bioavailability and drug-drug interactions. J Pharmacol Exp Ther. 2010;334 (3):1009–22.
27. Janneh O, Anwar T, Jungbauer C, Kopp S, Khoo SH, Back DJ, *et al.* P-glycoprotein, multidrug resistance-associated proteins and human organic anion transporting polypeptide influence the intracellular accumulation of atazanavir. Antivir Ther. 2009;14(7):965–74.
28. Dailly E, Tribut O, Tattevin P, Arvieux C, Perre P, Raffi F, *et al.* Influence of tenofovir, nevirapine and efavirenz on ritonavir-boosted atazanavir pharmacokinetics in HIV-infected patients. Eur J Clin Pharmacol. 2006;62(7):523–6.
29. Hubatsch I, Ragnarsson EG, Artursson P. Determination of drug permeability and prediction of drug absorption in Caco-2 monolayers. Nat Protoc. 2007;2(9):2111–9.
30. Hu Y, Smith DE, Ma K, Jappar D, Thomas W, Hillgren KM. Targeted disruption of peptide transporter Pept1 gene in mice significantly reduces dipeptide absorption in intestine. Mol Pharm. 2008;5(6):1122–30.
31. Jappar D, Wu SP, Hu Y, Smith DE. Significance and regional dependency of peptide transporter (PEPT) 1 in the intestinal permeability of glycylsarcosine: *in situ* single-pass perfusion studies in wild-type and Pept1 knockout mice. Drug Metab Dispos. 2010;38(10):1740–6.
32. Adachi Y, Suzuki H, Sugiyama Y. Quantitative evaluation of the function of small intestinal P-glycoprotein: comparative studies between *in situ* and *in vitro*. Pharm Res. 2003;20(8):1163–9.
33. Dahan A, Amidon GL. Segmental dependent transport of low permeability compounds along the small intestine due to P-glycoprotein: the role of efflux transport in the oral absorption of BCS class III drugs. Mol Pharm. 2009;6(1):19–28.
34. Masaoka Y, Tanaka Y, Kataoka M, Sakuma S, Yamashita S. Site of drug absorption after oral administration: assessment of membrane permeability and luminal concentration of drugs in each segment of gastrointestinal tract. Eur J Pharm Sci. 2006;29(3–4):240–50.
35. MacLean C, Moenning U, Reichel A, Fricker G. Closing the gaps: a full scan of the intestinal expression of p-glycoprotein, breast cancer resistance protein, and multidrug resistance-associated protein 2 in male and female rats. Drug Metab Dispos. 2008;36 (7):1249–54.
36. Zastre JA, Chan GN, Ronaldson PT, Ramaswamy M, Couraud PO, Romero IA, *et al.* Up-regulation of P-glycoprotein by HIV protease inhibitors in a human brain microvessel endothelial cell line. J Neurosci Res. 2009;87(4):1023–36.
37. Bousquet L, Roucairol C, Hembury A, Nevers MC, Creminon C, Farinotti R, *et al.* Comparison of ABC transporter modulation by atazanavir in lymphocytes and human brain endothelial cells: ABC transporters are involved in the atazanavir-limited passage across an *in vitro* human model of the blood–brain barrier. AIDS Res Hum Retrovir. 2008;24(9):1147–54.
38. Taipalensuu J, Tornblom H, Lindberg G, Einarsson C, Sjoqvist F, Melhus H, *et al.* Correlation of gene expression of ten drug efflux proteins of the ATP-binding cassette transporter family in normal human jejunum and in human intestinal epithelial Caco-2 cell monolayers. J Pharmacol Exp Ther. 2001;299(1):164–70.
39. Seithel A, Karlsson J, Hilgendorf C, Bjorquist A, Ungell AL. Variability in mRNA expression of ABC- and SLC-transporters in human intestinal cells: comparison between human segments and Caco-2 cells. Eur J Pharm Sci. 2006;28(4):291–9.
40. Hayeshi R, Hilgendorf C, Artursson P, Augustijns P, Brodin B, Dehertogh P, *et al.* Comparison of drug transporter gene expression and functionality in Caco-2 cells from 10 different laboratories. Eur J Pharm Sci. 2008;35(5):383–96.
41. Balimane PV, Chong S. A combined cell based approach to identify P-glycoprotein substrates and inhibitors in a single assay. Int J Pharm. 2005;301(1–2):80–8.
42. Zakeri-Milani P, Valizadeh H, Tajerzadeh H, Azarmi Y, Islambolchilar Z, Barzegar S, *et al.* Predicting human intestinal permeability using single-pass intestinal perfusion in rat. J Pharm Pharm Sci. 2007;10(3):368–79.
43. Karlgren M, Vildhede A, Norinder U, Wisniewski JR, Kimoto E, Lai Y, *et al.* Classification of inhibitors of hepatic organic anion transporting polypeptides (OATPs): influence of protein expression on drug-drug interactions. J Med Chem. 2012;55 (10):4740–63.
44. Konig J. Uptake transporters of the human OATP family: molecular characteristics, substrates, their role in drug-drug interactions, and functional consequences of polymorphisms. Handb Exp Pharmacol. 2011;201:1–28.
45. Glaeser H, Bailey DG, Dresser GK, Gregor JC, Schwarz UI, McGrath JS, *et al.* Intestinal drug transporter expression and the impact of grapefruit juice in humans. Clin Pharmacol Ther. 2007;81(3):362–70.
46. Meier Y, Eloranta JJ, Darimont J, Ismair MG, Hiller C, Fried M, *et al.* Regional distribution of solute carrier mRNA expression along the human intestinal tract. Drug Metab Dispos. 2007;35 (4):590–4.
47. Sai Y, Kaneko Y, Ito S, Mitsuoka K, Kato Y, Tamai I, *et al.* Predominant contribution of organic anion transporting polypeptide OATP-B (OATP2B1) to apical uptake of estrone-3-sulfate by human intestinal Caco-2 cells. Drug Metab Dispos. 2006;34 (8):1423–31.
48. Zapor MJ, Cozza KL, Wynn GH, Wortmann GW, Armstrong SC. Antiretrovirals, Part II: focus on non-protease inhibitor antiretrovirals (NRTIs, NNRTIs, and fusion inhibitors). Psychosomatics. 2004;45(6):524–35.

49. Tong L, Phan TK, Robinson KL, Babusis D, Strab R, Bhoopathy S, *et al.* Effects of human immunodeficiency virus protease inhibitors on the intestinal absorption of tenofovir disoproxil fumarate *in vitro*. Antimicrob Agents Chemother. 2007;51(10):3498–504.
50. Kearney BP, Flaherty JF, Shah J. Tenofovir disoproxil fumarate: clinical pharmacology and pharmacokinetics. Clin Pharmacokinet. 2004;43(9):595–612.
51. Nekvindova J, Masek V, Veinlichova A, Anzenbacherova E, Anzenbacher P, Zidek Z, *et al.* Inhibition of human liver microsomal cytochrome P450 activities by adefovir and tenofovir. Xenobiotica. 2006;36(12):1165–77.
52. Jayakanthan M, Chandrasekar S, Muthukumaran J, Mathur PP. Analysis of CYP3A4-HIV-1 protease drugs interactions by computational methods for highly active antiretroviral therapy in HIV/AIDS. J Mol Graph Model. 2010;28(5):455–63.
53. Wempe MF, Anderson PL. Atazanavir metabolism according to CYP3A5 status: an *in vitro-in vivo* assessment. Drug Metab Dispos. 2011;39(3):522–7.
54. Kile DA, Mawhinney S, Aquilante CL, Rower JE, Castillo-Mancilla JR, Anderson PL. A population pharmacokinetic-pharmacogenetic analysis of atazanavir. AIDS Res Hum Retroviruses. 2012;28(10):1227–34.